International Journal of Control and Automation
Vol.7, No.6 (2014), pp.43-50
http://dx.doi.org/10.14257/ijca.2014.7.6.05

Research in Turn-on Delay of Semiconductor Lasers

Jialing Wang, Ming Wang, Jia Lv and Shuai Huan
Basic Science College, Harbin University of Commerce, Harbin 150001 P. R. China
rainbowlgirl521@sina.com

Abstract

This paper derived out a closed expression describing the time evolution of the carrier density within the turn-on period of a semiconductor laser, for the case that the Auger effect is considered with a term which is proportional to the cube of the carrier density. As a result, an explicit analytical expression for the turn-on delay of the diode laser has also been deduced.

Keywords: *Semiconductor laser; Auger effect; Turn-on delay; Time evolution; Carrier density*

1. Introduction

Semiconductor laser works by incentives, the use of semiconductor material (both using electronic) transition between can shine in a semiconductor crystal cleavage plane form two parallel reflection mirror as a mirror, and form a resonant cavity, the oscillation, feedback, produce light amplification of radiation, the output laser. Semiconductor laser advantage is small size, light weight, reliable operation, less consumption, high efficiency, *etc.*

Nonradiative recombination (in particular, the Auger effect) and the carrier leakage over the hetero barrier have been reported theoretically as well as experimentally for 1.3 ym wavelength GaInAsP/InP crystals. Most of these works have concentrated on 1.3 pm lasers. As for 1.5-1.6 pm GaInAsP/InP crystals, the effects of the intervallic band absorption were reported, and the nonradiative recombination in relation to the carrier lifetime has been measured.

Auger effect is associated with an electron energy reduced at the same time, another higher electron energy transition process. Will launch photoelectron, auger electron (cannot be explained in the photoelectric effect) to atoms and molecules becomes a phenomenon known as auger effect ion of higher order. According to this effect made auger electron spectrometer, has been on the surface physical and chemical reaction kinetics, metallurgy, electron, *etc.*, within the territory of the high sensitivity of detection and rapid analysis. Auger effect is one of the atomic emission result in one or more other electronic (auger electron) is rather than the radiation emitted x-rays (explained in the photoelectric effect), the atoms and molecules become advanced ion physical phenomena, is associated with an electron energy reduced at the same time, the other one (or more) increased electron energy transition process. It named Auger effect because of the French Pierre Victor Auger.

In 1925, Pierre Victor Auger on the analysis of the Wilson cloud chamber found after the results of the experiment. Experiments using high energy X-rays to electronic gases, optoelectronics and observed. For electronic measurement shows that the trajectory has nothing to do with the frequency of the photon, this suggests that the mechanism is the atomic internal electronic ionization energy exchange or no radiation transition. Use of basic

ISSN: 2005-4297 IJCA

quantum mechanics to calculate the transition rate and the transition probability, and further experiments and theoretical studies has shown that the mechanism of this effect is no radiation transition, rather than the internal energy exchange.

As known a certain time is needed for the carrier density n to reach the threshold value nth when the bias of the semiconductor laser(LD) is suddenly changed from a below threshold current I0 to an above threshold current I, this time is known as turn-on delay [1] and will be denoted as td in this paper.

Since the turn-on delay is an important parameter of a semiconductor laser, intensified studies on this parameter have been carried out in the past years.

Researches [1-3] pointed out that the carrier dissipation F(n) of the InGaAsP LDs with a low doping level active layer working at 1.3 or 1.55 um can be described as

$$F(n) = An + Bn^2 + Cn^3 \tag{1}$$

Where n is the carrier density inside the diode, A, B and C are the non-radiative capture, radiative recombination and Auger coefficients, respectively.

To our knowledge, when the Auger effect can not neglected, the analytical expression for the turn-on delay has not been deduced. When one is in the inner electrons are removed, leaving a space, high energy level electrons will fill the vacancy, release energy at the same time. Usually in the form of emitted photons released energy, but also can launch an electron in atom to release. The second of emission electrons is called the Auger electron.

In this paper, the Auger effect was considered and the carrier rate equation within the turn-on delay period was integrated. As a result, a closed equation describing the time evolution of the carrier density before the LD is turned on was deduced. Further manipulation on this equation, an explicit analytical expression of td has been derived.

2. Study Backgrounds

Before the pump current I is applied to the LD at certain instant, say t=0, the carrier density n0 inside the diode satisfies[l] the Eq.(2):

$$I_0 = eVF(n_0) \tag{2}$$

Where e is the charge（absolute value）of an electron and V is the volume of the active layer. A pump carrier density N can be defined in the same way, as shown in Eq.(3).

$$I = eVF(N) \tag{3}$$

In physics, a one-to-one correspondence should exist between I and N, or I0 and n0. To obtain n0 or N from I0 or I, a cubic equation is involved. A standard method of solving the cubic equation can be found in mathematical manuals. Thus, both I0 and n0 can be regarded as the pre-bias, and I and N as pump. Although it is more convenient to use the current in practice, the two parameters are both effective [4].

During the turn-on delay period, the stimulated emission can be neglected and the carrier rate equation is following [1]

$$\frac{dn}{dt} = \frac{I}{eV} - F(n) \tag{4}$$

Inserting (1) and (3) into (4), one has

$$\frac{dn}{dt} = (N-n)\left[A + B(N+n) + C(N^2 + Nn + n^2)\right] \tag{5}$$

Letting y=N-n, Eq.(5) becomes

$$-\frac{dy}{dt} = y(Cy^2 - k_1 y + t_f) \tag{6}$$

Where $k_1 = (B+3CN)/2C = N + (B+CN)/2C$ and $t_f^{-1} = A + 2BN + 3CN^2 = dF(N)dN$

Quantity tf is named 'differential recombination time' [1] and similar to the virtual Lifetime [5]. After separating factors, Eq. (6) leads to

$$\frac{t}{t_f} = \int_{N-n}^{N-n_0} \left[\frac{1}{y} - \frac{(y-k_1)-k_1}{(y-k_1)^2 + {k_2}^2}\right] dy \tag{7}$$

With

$$k_2 = (4AC + 2BCN + 3CN^2 - B^2)^{1/2} / 2C$$

Integrating Eq. (7), one obtains

$$\begin{aligned} \frac{t}{t_f} &= \ln\frac{N-n_0}{N-n} + \ln\{[(n-N+k_1)^2 + {k_2}^2]/ \\ &[(n_0-N+k_1)^2 + {k_2}^2]\}/2 \\ &+(k_1/k_2)\text{arctg}\{k_1(n-n_0)/ \\ &[(n-N+k_1)(n_0-N+k_1) + {k_2}^2]\} \end{aligned} \tag{8}$$

Thus, the equation describing the time evolution of the carrier density during the turn-on delay period has been established. If one wants to know the time needed for the carrier density to reach certain level after the pump is applied, direct insertion of the required n into Eq. (8) gives the required time.

According to the definition of the turn-on delay [1], at time td the carrier density reaches nth, for the first time. Thus, from Eq. (8), the explicit analytical expression of t_d is

$$\begin{aligned} \frac{t_d}{t_f} &= \ln\frac{N-n_0}{N-n_{th}} + \ln\{[(n_{th}-N+k_1)^2 + {k_2}^2]/ \\ &[(n_0-N+k_1)^2 + {k_2}^2]\}/2 \\ &+(k_1/k_2)arctg\{k_1(n_{th}-n_0)/ \\ &[(n_{th}-N+k_1)(n_0-N+k_1) + {k_2}^2]\} \end{aligned} \tag{9}$$

From Eq. (9), one can see that if n0 goes to nth, td goes to zero. This indicates that the higher the pre-bias is, the shorter the turn-on delay will be. If the pre-bias is at the threshold,

the LD is in the oscillation regime already and certainly t_d is equal to zero. If N approaches n_{th}, the first term on the right of Eq.(8) goes to infinity. This means that a weak pump will result in a long turn-on process.

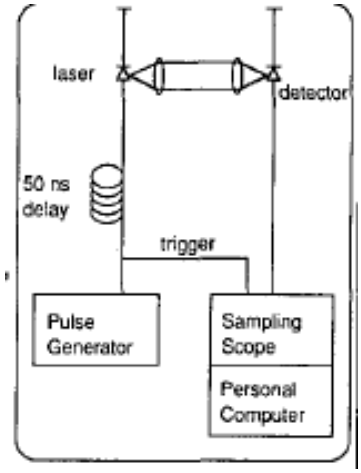

Figure 1. The inset shows the experimental setup for the jitter measurements

The laser is driven by the pulse generator and the optical pulses detected by a fast photo detector in conjunction with the sampling oscilloscope. The probability density function of the laser turn-on is measured by a personal computer that acts as a multichannel analyzer.

3. Calculations and Discussions

For the purpose of comparison, in the following we will give the expression of the turn- on delay td1, for the case of C=0. Denoting the differential recombination time as tf1, calculations lead to

$$\frac{t}{t_{f1}} = \ln\frac{N-n_0}{N-n} + \ln\frac{A/B+N+n}{A/B+N+n_0} \tag{10a}$$

$$\frac{t_{d1}}{t_{f1}} = \ln\frac{N-n_0}{N-n_{th}} + \ln\frac{A/B+N+n_{th}}{A/B+N+n_0} \tag{10b}$$

It should be pointed out that tf1 is still equal to the reciprocal of $dF(N)/dN$ when C equals zero.

Figure 2 shows time evolution of the carrier density $n(t)/n_{th}$, during the turn-on period where $n(t)/n_{th}$ is equal to 0, 0.25 and 0.5, respectively. In the calculations, $A=1\times10^{8}s^{-1}$, $B=1\times10^{-10}cm^3/s$, $C=3\times10^{-29}cm^6/s$, $N=2.5\times10^{18}cm^{-3}$, and $n_{th}=2\times10^{18}$. It should be noticed that the intersections of these curves with the top line of the frame give the turn-on delays for the respective pre-bias conditions. From the diagram it can be seen that a larger pre-bias may result in a shorter turn-on delay. It can also be observed that the carrier density increases at a

higher rate shortly after the pump is applied to the LD and then at a lower rate as n approaches n_{th}.

Figure 3 shows time evolution of the carrier density $n(t)/n_{th}$, during the turn-on period, where $C=2\times, 4\times$ and $6\times10^{-29} cm^6/s$, respectively. In the calculations, n0 is equal to zero and the other data are the same as those given in Figure 1.

This is mainly because the differential recombination time reduces with an increase in the Auger coefficient. From Eq.(8), it can be observed that the time is scaled at t_f, it is, therefore, understood that the turn-on process goes on at a faster rate than that anticipated when the Auger effect is neglected.

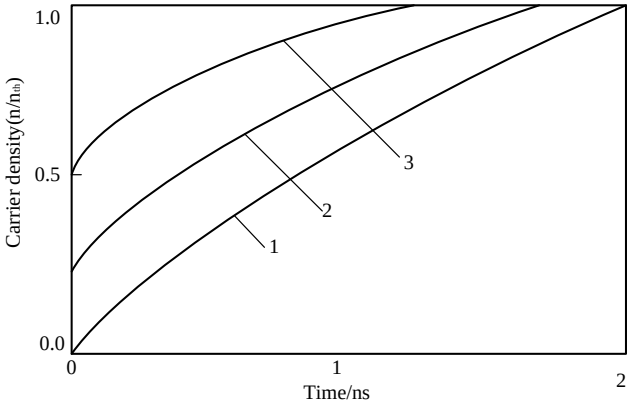

Figure 2. Time Evolution of Carrier Density

1: $n_0/n_{th}=0$*; 2:* $n_0/n_{th}=0.25$*; 3:* $n_0/n_{th}=0.5$

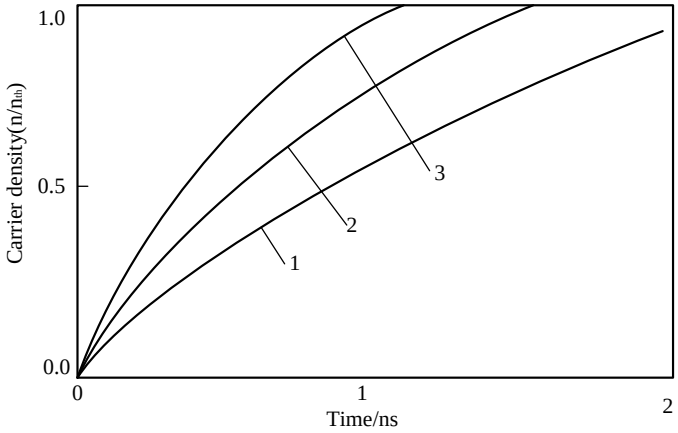

Figure 3. Time Evolution of Carrier Density

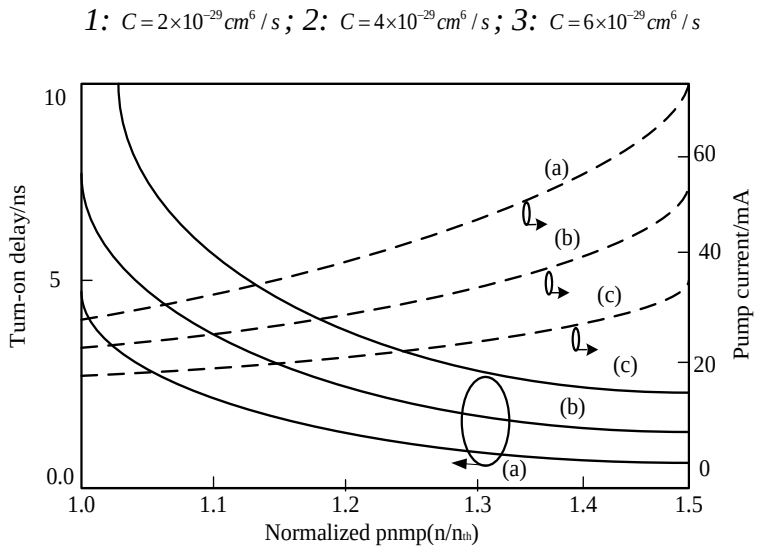

Figure 4. Dependence of turn-on delay (solid curves) on pump carrier density for time

Evolution of carrier C equal to (a) $6\times10^{-29}cm^6/s$, (b) $6\times10^{-29}cm^6/s$,(c) 0, repectively. Pump currents for respective carrier densities have also be shown(dashed curves) in Figure 3.

The pre-bias is zero and other data used to research the relationship of turn-on delay (solid curves) on pump carrier density for time are the same as those given above. The results are shown in Figure 4, from which one can see that the larger the pump is, the shorter the turn-on delay will be. Comparing the curves with C equal and not equal to zero, one can see that a larger Auger coefficient will result in a faster turn-on process. Since the same pump current does not relate to the same current if the Auger coefficient is different, the dashed curves is added into the Figure 3 to show the dependence of the current on the carrier density.

5. Conclusions

A closed expression describing the time evolution of the carrier density within the turn-on period of a semiconductor laser has been derived for the case that the Auger effect is considered with a term proportional to the cube of the carrier density. The equation obtained in this paper is verified using the data given in Ref. [1] and the test results are identical to those given in the same reference. The additional wavelength shift of the peak gain due to the inhomogeneous carrier distribution inside the LD has been calculated. It turns out that the shift is proportional to the mean square deviation of the carrier density from its mean value when the diode is above-threshold biased. After solving the traveling wave rate equations, it is determined that for the diode cited in this work the additional wavelength shift may approach the order of 0.1 nm under certain circumstances. This may affect the oscillation mode when the diode is operated in an external cavity with a length of tens of centimeters.

References

[1] L. B. Fu, M. Ibsen, D. J. Richardson, J. Nilsson, *et al*., "Compact High-Power Tunable-Level Operation of Double Cladding Nd-Doped Fiber Laser", IEEE Photon. Techno. Lett, vol. 172, **(2005)**, pp. 306-308.
[2] G. P. Agrawal and N. K. Dutta, "Semiconductor lasers", 2nd ed. Van Nostrand Reinhold, Sec. 6. 4. 2, New York, (**1993**) October.
[3] M. Asada and Y. Suematsu, "Measurement of spontaneous emission efficiency and nonradiative recomhinations in 1.58 um wavelength GaAlAsP/InP crystals", Appl. Phys. Lett., vol. 4, no. 41, **(1982).**
[4] G. Xia, Z. Wu and J. Chen, "Studying semiconductor lasers with multimode rate equations", Appl . Opt., vol. 34, no. 9, **(1995),** pp. 1523-1527.
[5] J. Wang, J. Chen and Y. Hao, "Additional wavelength shift of peak gain due to inhomogeneous distributions of carriers inside semiconductor lasers", IEEE Photonics Technol. Lett., vol. 5, no. 10, **(1993**), pp. 1171-1173.
[6] R. Selvas, J. K. Sahu, L. B. Fu, J. N. Jang, *et al*., "High-power, low-noise, Yb-doped, cladding-pumped, three-level fiber sources at 980nm", Optics letters, vol. 28, no. 13, **(2003)**, pp. 1093-1095
[7] P. D. Dragic, L. M. Little and G. C. Papen, "Fiber amplification in the 940-nm water vapor absorption band using the/sup 4/F/sub 3/2//sup 4/I/sub 9/2/transition in Nd", Photonics Technology Letters, IEEE, vol. 9, no. 11, **(1997)**, pp. 1478-1480.
[8] J. Dawson, R. Beach, A. Drobshoff, Z. Liao, *et al*., "938 nm Nd-doped high power cladding pumped fiber amplifier", Advanced Solid-State Photonics, OSA Technical Digest, (Optical Society of America, Washington, DC, **(2003)**, pp. 119-121.
[9] Gao, J. Yu, X. Chen, F. Li, *et al*., "12.0-W continuous-wave diode-end-pumped Nd: GdVO< sub> 4</sub> laser with high brightness operating at 912-nm. Optics Express", vol. 17, no. 5, **(2009)**, pp. 3574-3580.
[10] T. J. Kane, G. Keaton, M. A. Arbore, D. R. Balsley, *et al*., "3-Watt blue source based on 914-nm Nd: YVO4 passively-Q-switched laser amplified in cladding-pumped Nd: fiber", Proc. Advanced Solid-State Photonics, **(2004)**, pp. 2-5.
[11] A. L. Cook and H. D. Hendricks, "Diode-laser-pumped tunable 896–939.5-nm neodymium doped fiber laser with 43-mW output power", Applied optics, vol. 37, no. 15, **(1998)**, pp. 3276-3281.
[12] O. Svelto, S. Longhi, G. Della Valle, G. Huber, *et al*., "Lasers and coherent light sources", In Springer Handbook of Lasers and Optics, **(2012)**, pp. 641-1046.
[13] C. Y. Wang, H. H. Liu, S. Y. Chung, C. H. Teng, *et al*., "High-Accuracy Waveguide Leaky-Mode Analysis Using a Multidomain Pseudospectral Frequency-Domain Method Incorporated With Stretched Coordinate", PML. Journal of Lightwave Technology, vol. 31, no. 14, **(2013)**, pp. 2347**.**
[14] C. Sima, J. C. Gates, H. L. Rogers, P. L. Mennea, *et al*., "Ultra-wide detuning planar Bragg grating fabrication technique based on direct UV grating writing with electro-optic phase modulation", Optics express, vol. 21, no. 13, **(2013)**, pp. 15747-15754.
[15] N. Soleimani, B. Ponting, E. Gebremichael, A. Ribuot, *et al*., "Coilable Single Crystals Fibers of Doped-YAG for High Power Laser Applications", Journal of Crystal Growth, **(2013).**
[16] Y. S. Liu , T. C. Galvin, T. Hawkins, J. Ballato, *et al*., "Linkage of oxygen deficiency defects and rare earth concentrations in silica glass optical fiber probed by ultraviolet absorption and laser excitation spectroscopy", Optics Express, vol. 20, no. 13, **(2012)**, pp. 14494-14507.
[17] A. Pal, R. Sen, K. Bremer, S. Yao, *et al*., "All-fiber tunable laser in the 2 μm region, designed for CO 2 detection", Applied optics, vol. 51, no. 29, **(2012)**, pp. 7011-7015.

